

Deep tremor in New Zealand triggered by the 2010 Mw8.8 Chile earthquake

B. Fry,¹ K. Chao,² S. Bannister,¹ Z. Peng,² and L. Wallace¹

Received 31 May 2011; revised 23 June 2011; accepted 28 June 2011; published 9 August 2011.

[1] Deep non-volcanic tremor (NVT) is usually associated with episodic slow-slip events. New Zealand is one notable exception where numerous slow slip events have been identified, yet NVT has remained undetected. Here we present the first known case of triggered NVT at New Zealand's Hikurangi subduction margin. Following the Mw8.8 Chilean earthquake of February 27, 2010, we identify coherent high-frequency tremor signals that are in phase with, and modulated by, the passing Rayleigh waves. This is consistent with the surface wave triggering potential for strike-normal incidence on a low-angle thrust fault. After constraining the tremor depth on the plate interface, we locate the tremor source within 20 km of the source area of episodic slow slip. The tremor location is also near the edge of a region with high seismic attenuation that marks the boundary between dehydrated subducted slab and inferred hydrated, underplated sediment. We speculate that reduced interface friction and high fluid pressures provided by fluid-rich underplated sediment facilitates the tremor generation. **Citation:** Fry, B., K. Chao, S. Bannister, Z. Peng, and L. Wallace (2011), Deep tremor in New Zealand triggered by the 2010 Mw8.8 Chile earthquake, *Geophys. Res. Lett.*, 38, L15306, doi:10.1029/2011GL048319.

1. Introduction

[2] Subduction interface earthquakes account for 9 of the 10 largest earthquakes since 1900 (http://earthquake.usgs.gov/earthquakes/world/10_largest_world.php). Consequently, the contribution of subduction thrust earthquakes to seismic hazard in regions proximal to subduction zones is large. The exciting discovery over the last decade of slow slip events (SSEs) and non-volcanic tremor (NVT) occurring on subduction plate interfaces worldwide has elucidated the broad spectrum of subduction thrust slip behavior [e.g., Peng and Gomberg, 2010; Beroza and Ide, 2011]. SSEs and NVT are typically observed in the downdip transition from the locked, seismogenic portion of the plate interface to the aseismically creeping portion of the interface. Understanding the continuum of subduction thrust fault deformation is necessary for accurate knowledge of the stress regime and physical conditions on the plate interface, and for a better understanding of the hazard posed by these major processes.

[3] In many subduction zones where slow slip has been identified, NVT is present and appears to be spatially and temporally related to slow slip. The Hikurangi Subduction

Margin, New Zealand is one notable exception, where numerous SSEs have been identified [Wallace and Beavan, 2010] yet the detection of NVT has remained elusive. The Hikurangi Margin marks the convergent plate boundary where the Hikurangi Plateau, part of the Pacific plate, subducts beneath the eastern North Island at 2–6 cm/yr [Wallace et al., 2004]. Although no subduction earthquakes larger than Mw 7.2 have been recorded in New Zealand since the development of modern seismographs, geological evidence suggests that the overriding plate is prone to large vertical displacements [Cochran et al., 2006; Hayward et al., 2006] that are commonly interpreted as evidence for great megathrust events [e.g., Clague, 1997; Cisternas et al., 2005]. Numerous slow-slip events have been observed in New Zealand down-dip from the interseismically locked regions on the plate interface [McCaffrey et al., 2008; Wallace and Beavan, 2010, and references therein]. The occurrence of New Zealand SSEs at the downdip transition from interseismic coupling to aseismic creep fits the conceptual model of continuum deformation in which slow-slip events and regular earthquakes are end members differentiated by the fault's frictional properties and rate of slip, and consequently, the frequency of radiated seismic energy [e.g., Peng and Gomberg, 2010].

[4] To date, there has been no conclusive evidence of tremor in New Zealand. Delahaye et al. [2009] conducted a systematic search but failed to find any tremor signals in association with documented slow-slip events at the northern Hikurangi margin (Figure 1). Instead, they found that a slow-slip episode in 2004 was accompanied by numerous reverse-faulting microearthquakes, similar to the microseismicity associated with SSEs on the subduction interface near Boso Peninsula in central Japan (Sagiya, 2004) [Ozawa et al., 2007]. It is worth noting that the SSEs associated with microearthquakes [Delahaye et al., 2009] are at <15 km depth, just downdip of a region of unusually shallow interseismic locking [Wallace and Beavan, 2010]. Elsewhere, most subduction zones with well-documented NVT have much deeper interseismic coupling and slow slip events, and the tremor in many of these locations occurs at 30–40 km depth [e.g., Shelly et al., 2006; La Rocca et al., 2009]. SSEs occurring at the southern and central part of the Hikurangi margin are observed deeper (>25 km depth) than in the north (Figure 1). The area around these deeper SSEs area could be a more fruitful hunting ground for tremor.

[5] In addition to commonly accompanying slow-slip events, recent studies have shown that tremor can be triggered instantaneously during large-amplitude surface waves of distant earthquakes [Peng and Gomberg, 2010, and reference therein]. Such triggered tremor is relatively easy to identify, as such tremor has a relatively high signal-to-noise ratio and a periodicity linked to surface waves. Here we conduct a systematic search for triggered tremor signals in

¹GNS Science, Lower Hutt, New Zealand.

²School of Earth and Atmospheric Sciences, Georgia Institute of Technology, Atlanta, Georgia, USA.

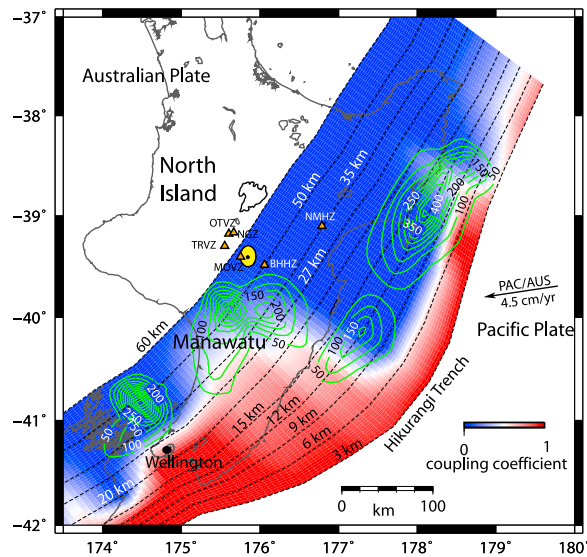


Figure 1. Tectonic setting of the Hikurangi subduction margin. The yellow ellipse shows the location of triggered tremor in relation to interseismic coupling and slow slip events on the subduction interface. Blue to red shading shows the degree of interseismic coupling on the Hikurangi subduction interface in terms of a coupling coefficient (blue = steady aseismic creep, red = full interseismic coupling); green contours show total slip (in mm) detected in SSEs on the Hikurangi subduction interface since 2002 [adapted from *Wallace and Beavan, 2010*]. Dashed black line shows depth contours (labeled) to the subduction interface. Black arrow labeled “PAC/AUS” shows the motion of the Pacific Plate relative to the Australian Plate in the North Island region [from *Beavan et al., 2002*]. Black arrow labeled EQ backaz shows the direction of prograde Rayleigh wave particle motion.

New Zealand in the time period immediately following the 2010/02/27 Mw8.8 Maule (Chile) earthquake. We focus on this particular earthquake because of its long rupture duration and relatively shallow depth, which contributed to the generation of large amplitude surface waves in New Zealand. The Chile mainshock elsewhere triggered clear tremor and microearthquakes in Central California [*Peng et al., 2010*] and the Mexico subduction zone [*Zigone et al., 2010*]. In this study we present evidence for dynamically triggered tremor in the North Island of New Zealand, and discuss its spatial relationship with the location of slow slip events along the Hikurangi subduction margin.

2. Triggered Tremor Observations

[6] We identify triggered tremor following the procedure of *Peng et al. [2009]* and *K. Chao et al. (Remote triggering of non-volcanic tremor around Taiwan, submitted to *Geophysical Journal International*, 2011)*. We use all available stations (Figure S1 of the auxiliary material) from GeoNet—the New Zealand National Seismic Network [*Petersen et al., 2011*] in the North Island that recorded the Chile main shock.¹ We first remove the mean and instrument response,

¹Auxiliary materials are available in the HTML. doi:10.1029/2011GL048319.

and cut the data to 1000 s before and 9000 s after the origin time of the Chile mainshock, then generate a 2–8 Hz band-pass-filtered waveform and envelope functions. We visually identify tremor as high-frequency (2–8 Hz), long-duration, and non-impulsive seismic signals occurring during the large-amplitude surface waves. Figure 2 shows a comparison of the broadband and 2–8 Hz band-pass filtered data at station TRVZ. Clear high-frequency signals accompany, and appear to be modulated by, the long-period surface waves. The phase of the tremor envelope is most closely aligned to the phase of the Rayleigh wave as recorded in the radial direction (Figure 2). The tremor signals are strongest on the radial and transverse components. The tremor signals between 2200 and 2400 s are coherent among stations within 100 km (Figure 3 and Figure S2 of the auxiliary material) for most of the stations (excluding BKZ and WATZ). The observed tremor appears to be initiated by the long-period Rayleigh wave at around 2250 s, and then continues to be modulated by the subsequent short-period Rayleigh waves (Figure 2 and Figures S2, S3, and S4 of the auxiliary material). Long-period Love waves arrive between 2050 and 2150 s but no clear tremor is observed during this time window.

[7] We use a standard envelope cross-correlation technique [*Peng and Chao, 2008*] to obtain the tremor location by minimizing the root mean square (RMS) residuals between the theoretical *S*-wave travel time differences among station pairs and travel time differences observed from cross-correlating band-pass-filtered envelope functions. The theoretical *S*-wave travel times are computed based on an average 1D velocity model (Table S1 of the auxiliary material) derived from a nationwide 3D model [*Eberhart-Phillips et al., 2010*]. The best fitting location is longitude $175.85 \pm 0.15^\circ$, latitude $-39.40 \pm 0.20^\circ$ (Figure S1

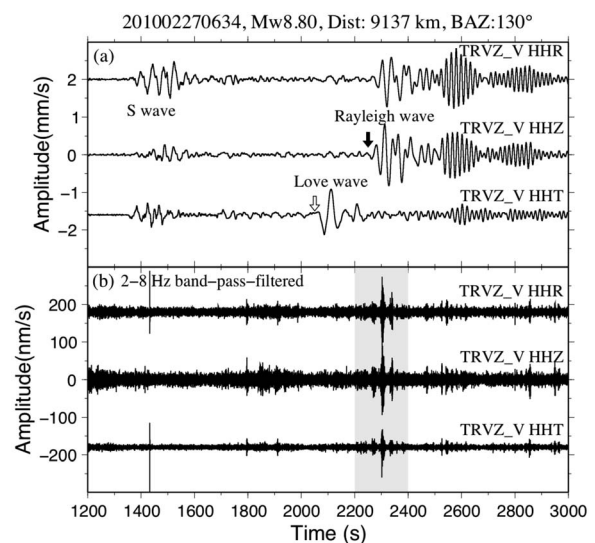


Figure 2. A comparison of the (a) broadband and (b) 2–8 Hz band-pass-filtered seismograms on radial (R), vertical (Z), and transverse (T) components at station TRVZ. The open and solid arrows mark the approximate arrival times of the Love and Rayleigh waves, respectively. The shaded area in Figure 2b marks the time of the triggered tremor during the long-period Rayleigh waves.

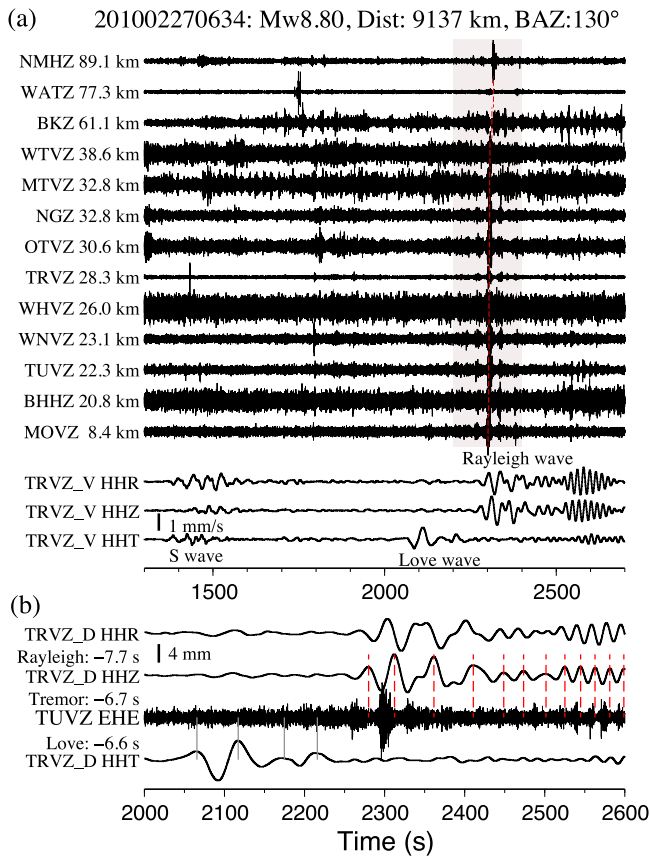


Figure 3. (a) 2–8 Hz band-pass-filtered seismograms on the east (E) component, showing the moveout of tremor between 2200 and 2400 s (shaded area) triggered by the 2010 Mw8.8 Chile earthquake. The seismograms are plotted with increasing hypocentral distance to the best-fitting tremor location (175.85°E, 39.40°S, 50 km) in the North Island. The red line marks the predicted *S*-wave arrival time at each station. The lower panel shows the radial (R), vertical (Z), and transverse (T) component velocity (V) seismograms recorded at station TRVZ. (b) A detailed comparison between the displacement (D) seismograms at TRVZ and the 2–8 Hz band-pass-filtered E component seismogram recorded at TUVZ. The vertical gray and red lines mark the peak of Love and Rayleigh waves, respectively. Each seismogram has been time-shifted back to the tremor occurrence time.

of the auxiliary material). As was found in previous studies [e.g., Rubinstein *et al.*, 2009], depths obtained from the envelope techniques are poorly constrained. Hence we project the tremor to the plate interface [Ansell and Bannister, 1996] and set the tremor depth at 50 km.

3. Relationship of Triggered Tremor to Slow Slip and Subduction Margin Structure

[8] As shown in Figure 1, our triggered tremor source lies at the northern edge of the source area of the 2004–2005 Manawatu SSE, which involved slip on the subduction interface from roughly 70 km depth to about 20 km [Wallace and Beavan, 2006, 2010]. That SSE occurred on the subduction interface close to the along-strike transition

change from deep to shallow interseismic coupling, determined from campaign GPS measurements [Wallace *et al.*, 2004]. CGPS data in the central North Island region indicates that a repeat of the 2004/2005 Manawatu event is currently underway, with more rapid than normal eastward movement of CGPS sites since late 2009/early 2010 [Wallace and Beavan, 2010]. Thus, although the NVT we discuss here was triggered by the 2010 Chile event, it also occurred adjacent to an area of ongoing slow slip.

[9] The Manawatu SSEs have relatively long durations (1–2 years), and involve slip on the interface equivalent to an Mw7.0 earthquake [Wallace and Beavan, 2006; Wallace and Beavan, 2010]. The duration, magnitude, and depth characteristics of the Manawatu events are similar to the Bungo Channel SSEs and Tokai SSEs observed in central and southwest Japan [Obara and Hirose, 2006], and the long-term slow-slip events in central Mexico [Kostoglodov *et al.*, 2010]. In these areas, NVT tends to occur adjacent to and in the deeper portion of the long-term SSE source area [Obara and Hirose, 2006; Kato *et al.*, 2010], similar to what we observe for the location of the triggered NVT relative to the Manawatu SSE source area. In cases where SSE events are shorter in duration (e.g., <1–2 months), tremor appears to coincide more closely with the location of the SSE source area [e.g., Hirose and Obara, 2006; Obara and Hirose, 2006; Gomberg *et al.*, 2010]. The location of tremor at the periphery of long-lived, large SSEs (such as Manawatu, central Mexico, Bungo Channel, and Tokai) is likely informing us about spatial variations in frictional conditions and fluid pressures on the subduction interface in those regions.

[10] The observed tremor is also located within an area of high seismic attenuation (low *Q*) above the subduction interface (Figure 4) that has previously been interpreted as hydrated underplated sediments [Eberhart-Phillips *et al.*, 2008]. Fluids from devolatilization of the subducted slab may also infiltrate the underplated sediments in this region, contributing to a discontinuity in physical state between the dehydrated, rigid slab and overriding plate [Eberhart-Phillips *et al.*, 2008]. Although the slab itself is dehydrated and may behave in a brittle fashion, the presence of abundant fluid-rich underplated sediment overlying the slab promotes high fluid

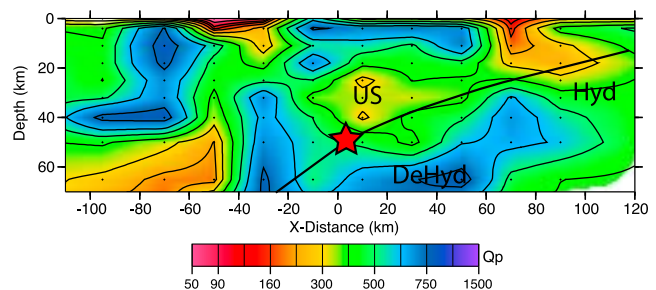


Figure 4. Cross section showing *Q_p* (inverse of seismic attenuation) and interpretations [Eberhart-Phillips *et al.*, 2008] at the Hikurangi Subduction Margin. The red star shows the best-fitting location of the tremor source. The solid black line marks the plate interface. Interpretations of *Q_p* by Eberhart-Phillips *et al.* [2008] include US: underplated sediments, hyd: hydrated material, and DeHyd: dehydrated material.

pressures on the subduction interface, possibly creating a favorable situation for tremor occurrence. At other subduction zones it has been noted that tremor locations tend to coincide with high V_p/V_s ratios, and this has been used to infer high pore fluid pressures in regions of slow slip and tremor [Shelly *et al.*, 2006; Audet *et al.*, 2009; Kato *et al.*, 2010], leading to the suggestion that high fluid pressures play an important role in the generation of NVT and SSEs [Peng and Gomberg, 2010; Beroza and Ide, 2011].

4. Discussion

[11] We have identified 2–8 Hz signal in New Zealand during the teleseismic waves of the Mw8.8 Chile earthquake of February 27, 2010. We interpret this signal as NVT resulting from movement on the Hikurangi subduction interface as the boundary is dynamically stressed by the incoming Rayleigh waves. In comparison, the Love wave, with comparable amplitude, did not appear to trigger any tremor signals above the background noise. The relative plate motion between the Australian and Pacific plate in this region is approximately 3.5 cm/year at about 220 degrees [Beavan *et al.*, 2002]. The surface waves arrive in New Zealand after travelling approximately ~9100 km along a back-azimuth (BAZ) of about 130 degrees, leading to an incidence nearly perpendicular to strike of the subduction zone, and about 45 degrees away from the Australia/Pacific plate motion vector (Figure 1) Recently, Hill [2010] conducted a systematic modeling of the surface wave potential for triggering deep tremor, based on the Coulomb failure criterion. He found that for low-angle thrust fault and strike-normal incidence, the Rayleigh wave triggering potential is high while the Love wave triggering potential is null, consistent with our observation. The vertical peak ground velocities recorded at nearby broadband stations are on the order of 0.1 cm/s. Assuming a nominal phase velocity of 3.5 km/s and a shear rigidity of 35 GPa, this corresponds to a maximum dynamic stress of 10 kPa, close to the apparent triggering threshold found at other places [Peng *et al.*, 2009; K. Chao *et al.*, submitted manuscript, 2011]. Hence, triggered tremor in the Hikurangi subduction interface is likely to be similar to observations of triggered tremor elsewhere [Miyazawa *et al.*, 2008; Rubinstein *et al.*, 2009; Peng *et al.*, 2009; K. Chao *et al.*, submitted manuscript, 2011].

[12] The location of the tremor source is adjacent to the source area of repeated SSEs, suggesting that it may be related to the transition from seismic to aseismic slip on the interface. Although no NVT has been previously recognized in this region of episodic slow slip, our observation of triggered tremor here suggests that the physical conditions are favourable for production of NVT. The occurrence of triggered tremor may also be influenced by the presence of hydrated, underplated sediments that were previously subducted at Hikurangi trough (Figure 4).

[13] The S -wave travel times predicted from the best-fitting locations match well with the high-frequency signals observed at most stations, but not at stations BKZ and WATZ (Figure 3 and Figure S2 of the auxiliary material). In particular, the high-frequency signals at station BKZ appear to be well modulated by the surface waves (Figure S5 of the auxiliary material), suggesting that they are likely generated by another tremor source near station BKZ. Unfortunately, we did not find any additional stations that recorded signals

similar to those at station BKZ. Hence, we were unable to locate the source. In addition, it is worth noting that other groups have started to identify deep tremor activity in the North Island, and their initial locations are close to ours (A. Wech, personal communication, 2010), consistent with the inference that triggered tremor reflects accelerated driving of tremor by dynamic stress [Gomberg, 2010]. It is still not clear whether additional large teleseismic events have triggered tremor in the same region, or at multiple places in New Zealand, which we are currently investigating.

[14] **Acknowledgments.** We thank Donna Eberhart-Phillips for providing the Qp cross-section. The reviews of Mario La Rocca and an anonymous reviewer lead to an improved manuscript. Some figures were created with GMT [Wessel and Smith, 1995]. Z.P. and K.C. are supported by US National Science Foundation EAR-0956051.

[15] The Editor thanks Mario La Rocca and an anonymous reviewer for their assistance in evaluating this paper.

References

- Ansell, J., and S. Bannister (1996), Shallow morphology of the subducted Pacific Plate along the Hikurangi margin, New Zealand, *Phys. Earth Planet. Inter.*, 93(1–2), 3–20, doi:10.1016/0031-9201(95)03085-9.
- Audet, P., M. Bostock, N. Christensen, and S. Peacock (2009), Seismic evidence for overpressured subducted oceanic crust and megathrust fault sealing, *Nature*, 457, 76–78, doi:10.1038/nature07650.
- Beavan, J., P. Tregoning, M. Bevis, T. Kato, and C. Meertens (2002), Motion and rigidity of the Pacific Plate and implications for plate boundary deformation, *J. Geophys. Res.*, 107(B10), 2261, doi:10.1029/2001JB000282.
- Beroza, G., and S. Ide (2011), Slow earthquakes and nonvolcanic tremor, *Annu. Rev. Earth Planet. Sci.*, 39, 271–296, doi:10.1146/annurev-earth-040809-152531.
- Cisternas, M., *et al.* (2005), Predecessors of the giant 1960 Chile earthquake, *Nature*, 437, 404–407, doi:10.1038/nature03943.
- Clague, J. (1997), Evidence for large earthquakes at the Cascadia subduction zone, *Rev. Geophys.*, 35, 439–460, doi:10.1029/97RG00222.
- Cochran, U., *et al.* (2006), Paleocological insights into subduction zone earthquake occurrence, eastern North Island, New Zealand, *Geol. Soc. Am. Bull.*, 118, 1051–1074, doi:10.1130/B25761.1.
- Delahaye, E., J. Townend, M. Reyners, and G. Rogers (2009), Microseismicity but no tremor accompanying slow-slip in the Hikurangi subduction zone, New Zealand, *Earth Planet. Sci. Lett.*, 277, 21–28, doi:10.1016/j.epsl.2008.09.038.
- Eberhart-Phillips, D., M. Reyners, M. Chadwick, and G. Stuart (2008), Three-dimensional attenuation structure of the Hikurangi subduction zone in the central North Island, New Zealand, *Geophys. J. Int.*, 174, 418–434, doi:10.1111/j.1365-246X.2008.03816.x.
- Eberhart-Phillips, D., M. Reyners, S. Bannister, M. Chadwick, and S. Ellis (2010), Establishing a versatile 3-D seismic velocity model for New Zealand, *Seismol. Res. Lett.*, 81(6), 992–1000, doi:10.1785/gssrl.81.6.992.
- Gomberg, J. (2010), Lessons from (triggered) tremor, *J. Geophys. Res.*, 115, B10302, doi:10.1029/2009JB007011.
- Gomberg, J., *et al.* (2010), Slow-slip phenomena in Cascadia from 2007 and beyond: A review, *GSA Bull.*, 122(7–8), 963–978, doi:10.1130/B30287.1.
- Hayward, B., H. Grenfell, A. Sabaa, R. Carter, U. Cochran, J. Lipps, P. Shane, and M. Morley (2006), Micropaleontological evidence of large earthquakes in the past 7200 years in southern Hawke's Bay, New Zealand, *Quat. Sci. Rev.*, 25, 1186–1207, doi:10.1016/j.quascirev.2005.10.013.
- Hill, D. (2010), Surface-wave potential for triggering tectonic (nonvolcanic) tremor, *Bull. Seismol. Soc. Am.*, 100, 1859–1878, doi:10.1785/0120090362.
- Hirose, H., and K. Obara (2006), Short-term slow slip and correlated tremor episodes in the Tokai region, central Japan, *Geophys. Res. Lett.*, 33, L17311, doi:10.1029/2006GL026579.
- Kato, A., *et al.* (2010), Variations of fluid pressure within the subducting oceanic crust and slow earthquakes, *Geophys. Res. Lett.*, 37, L14310, doi:10.1029/2010GL043723.
- Kostoglodov, V., A. Husker, N. M. Shapiro, J. S. Payero, M. Campillo, N. Cotte, and R. Clayton (2010), The 2006 slow slip event and nonvol-

- canic tremor in the Mexican subduction zone, *Geophys. Res. Lett.*, *37*, L24301, doi:10.1029/2010GL045424.
- La Rocca, M., K. C. Creager, D. Galluzzo, S. D. Malone, J. E. Vidale, J. R. Sweet, and A. G. Wech (2009), Cascadia tremor located near plate interface constrained by S minus P wave times, *Science*, *323*, 620–623, doi:10.1126/science.1167112.
- McCaffrey, R., L. Wallace, and J. Beavan (2008), Slow slip and frictional transition at low temperature at the Hikurangi subduction zone, *Nat. Geosci.*, *1*, 316–320, doi:10.1038/ngeo178.
- Miyazawa, M., E. Brodsky, and J. Mori (2008), Learning from dynamic triggering of low-frequency tremor in subduction zones, *Earth Planets Space*, *60*, e17–e20.
- Obara, K., and H. Hirose (2006), Non-volcanic deep low-frequency tremors accompanying slow-slips in southwest Japan subduction zone, *Tectonophysics*, *417*, 33–51, doi:10.1016/j.tecto.2005.04.013.
- Ozawa, S., H. Suito, and M. Tobita (2007), Occurrence of quasi-periodic slow slip off the east coast of the Boso peninsula, central Japan, *Earth Planets Space*, *59*, 1241–1245.
- Peng, Z., and K. Chao (2008), Non-volcanic tremor beneath the Central Range in Taiwan triggered by the 2001 Mw 7.8 Kunlun earthquake, *Geophys. J. Int.*, *175*, 825–829, doi:10.1111/j.1365-246X.2008.03886.x.
- Peng, Z., and J. Gomberg (2010), An integrated perspective of the continuum between earthquakes and slow-slip phenomena, *Nat. Geosci.*, *3*, 599–607, doi:10.1038/ngeo940.
- Peng, Z., J. Vidale, A. Wech, R. Nadeau, and K. Creager (2009), Remote triggering of tremor along the San Andreas Fault in central California, *J. Geophys. Res.*, *114*, B00A06, doi:10.1029/2008JB006049.
- Peng, Z., D. P. Hill, D. R. Shelly, and C. Aiken (2010), Remotely triggered microearthquakes and tremor in central California following the 2010 Mw8.8 Chile earthquake, *Geophys. Res. Lett.*, *37*, L24312, doi:10.1029/2010GL045462.
- Petersen, T., K. Gledhill, M. Chadwick, N. Gale, and J. Ristau (2011), The New Zealand national seismic network, *Seismol. Res. Lett.*, *82*, 9–20, doi:10.1785/gssrl.82.1.9.
- Rubinstein, J., J. Gomberg, J. E. Vidale, A. G. Wech, H. Kao, K. C. Creager, and G. Rogers (2009), Seismic wave triggering of nonvolcanic tremor, episodic tremor and slip, and earthquakes on Vancouver Island, *J. Geophys. Res.*, *114*, B00A01, doi:10.1029/2008JB005875.
- Shelly, D., G. C. Beroza, S. Ide, and S. Nakamura (2006), Low-frequency earthquakes in Shikoku, Japan and their relationship to episodic tremor and slip, *Nature*, *442*, 188–191, doi:10.1038/nature04931.
- Wallace, L., and J. Beavan (2006), A large slow slip event on the central Hikurangi subduction interface beneath the Manawatu region, North Island, New Zealand, *Geophys. Res. Lett.*, *33*, L11301, doi:10.1029/2006GL026009.
- Wallace, L., and J. Beavan (2010), Diverse slow slip behavior at the Hikurangi subduction margin, New Zealand, *J. Geophys. Res.*, *115*, B12402, doi:10.1029/2010JB007717.
- Wallace, L., J. Beavan, R. McCaffrey, and D. Darby (2004), Subduction zone coupling and tectonic block rotations in the North Island, New Zealand, *J. Geophys. Res.*, *109*, B12406, doi:10.1029/2004JB003241.
- Wessel, P., and W. H. F. Smith (1995), New version of the Generic Mapping Tools released, *Eos Trans. AGU*, *76*(33), 329, doi:10.1029/95EO00198.
- Zigone, D., M. Campillo, A. L. Husker, V. Kostoglodov, J. S. Payero, W. Frank, N. M. Shapiro, C. Voisin, G. Cougoulat and N. Cotte (2010), Complex non-volcanic tremor in Guerrero Mexico triggered by the 2010 Mw 8.8 Chilean earthquake, Abstract S23A-2107 presented at 2010 Fall Meeting, AGU, San Francisco, Calif., 13–17 Dec.

S. Bannister, B. Fry, and L. Wallace, GNS Science, 1 Fairway Dr., Avalon, PO Box 30368, Lower Hutt 5040, New Zealand. (b.fry@gns.cri.nz)
 K. Chao and Z. Peng, School of Earth and Atmospheric Sciences, Georgia Institute of Technology, Atlanta, GA 30332, USA.